energies

MDPI

Article

Shear Resistance Properties of Modified Nano-SiO_2/AA/AM Copolymer Oil Displacement Agent

Nanjun Lai [1,2,*], Xin Guo [1], Ning Zhou [1] and Qian Xu [1]

[1] School of Chemistry and Chemical Engineering of Southwest Petroleum University, Chengdu 610500, China; 13558692597@163.com (X.G.); ning9409@hotmail.com (N.Z.); 13032832276@163.com (Q.X.)

[2] Faculty of Engineering and Applied Science, University of Regina, Regina, SK S4S 0A2, Canada

* Correspondence: lainanjun@126.com; Tel.: +86-28-83037306

Academic Editor: Alireza Bahadori

Received: 7 October 2016; Accepted: 22 November 2016; Published: 9 December 2016

Abstract: To address the problem regarding poor shear resistance of commonly employed polymers for oil displacement, modified nano-SiO_2/AA/AM copolymer (HPMNS) oil displacement agents were synthesized using acrylic acid (AA), acrylamide (AM), and modified nano-SiO_2 of different modification degrees as raw materials. HPMNS was characterized by means of infrared spectroscopy (IR), nuclear magnetic resonance (^{1}H-NMR, ^{13}C-NMR), dynamic/static light scattering, and scanning electron microscope. A comparative study of the shear resistance properties for partially hydrolyzed polyacrylamide (HPAM) and HPMNS was conducted. Compared to HPAM, the introduced hyperbranched structure endowed HPMNS with good shear resistance, which was quantified from the viscosity retention ratio of the polymer solutions. From the perspective of rheological property, HPMNS also showed great shear stability after shearing by a Mixing Speed Governor and porous media shear model. Furthermore, with a higher degree of modification, HPMNS-2 had better shear stability in terms of viscosity and rheological property than HPMNS-1. The phenomena were due to its lower hydrodynamic radius, weight-average molecular weight, and better flexibility of its molecular chains. In addition, upon the indoor displacement test, the resistance factor and residual resistance factor values of HPMNS-2 were higher than those of HPAM. This behavior is beneficial for increasing oil recovery.

Keywords: the modified nano-SiO_2/AA/AM copolymer; modification degrees; shear resistance; rheological property; enhanced oil recovery

1. Introduction

Polymer flooding is an important technology to extend oilfield life and increase oilfield production [1–8]. As the most commonly used polymer in field applications, a small quantity of partially hydrolyzed polyacrylamide (HPAM) can increase the viscosity of water by 2 or more orders of magnitude in the absence of added electrolytes because of the extremely high molecular weight and the repulsion between the negative charges along the polymer chain [9]. Employing polymer flooding for enhancement of oil recovery has major advantages, but also considerable drawbacks [10]. One such drawback is the lack of stability in terms of viscous and viscoelastic properties of HPAM caused by shearing actions of the stirrer, pipeline valve, injection pump, shot hole, and porous media during preparation and injection of polymer solution. One of the most common and obvious effects of this instability is significantly reduced viscosity of HPAM solutions when its linear architecture undergoes such scission, thus seriously reducing its ability to enhance oil recovery [8,10–16].

Several different polymeric topologies have been explored for their chain scission resistance characteristics, and such efforts largely appear to have been directed by availability of the architecture. For example, branching or grafting side chains to polymeric backbones is considered to enhance shear stability. However, grafting onto polymeric backbones may enhance the tensile stresses due to the additional drag on the grafts, and thus reduce shear stability [14].

With multiple linear chains linked to a single core, hyperbranched polymers have an elementary branching topology, which could enhance shear resistance. This is attributed to sacrificial scission of the branches, leading to only a small decrease in molecular weight. Currently, organics are usually used as cores to synthesize hyperbranched polymers [17–20], but they cannot effectively increase the number of branched chains on the premise of meeting the requirement for injection. Inorganic nano-SiO_2 is of small grain size, and has an internal three-dimensional, reticular, rigid structure, with many highly active Si–OH radical groups on its surface [21]. Prior researchers have introduced nano-SiO_2 into oil-displacing polymers by means of surface modification [9,22–25]. Pu et al. [23] synthesized novel water-soluble core-shell hyperbranched polymers (HBPAMs), consisting of nano-SiO_2 as the core, hyperbranched polyamidoamine (PAMAM) as the subshell, and linear hydrophilic chains as the outermost layer. Static experiments convincingly proved that the three-dimensional morphology endowed HBPAMs with excellent shear degradation resistance. The author's research group has synthesized a hybrid hyperbranched polymer based on nano-SiO_2, modified by 3-(trimethoxysilyl)-1-propanamine and maleic anhydride, successively [25].

By varying the numbers of functionalized branch-cell units, the numbers of outmost linear hydrophilic chains can be tuned, which will affect the copolymer's shear resistance [23]. Consequently, the primary objective of this study was to: (1) synthesize two copolymers with different degrees of modification by using the previously synthesized polymerizable modified nano-SiO_2 monomers [25] as the core; and (2) determine the shear resistance of the copolymers and the impact of the modification degree on the shear resistance. With the purpose of simulating the shearing actions the occur during preparation and injection in practice, the shearing resistance of the copolymer solutions were evaluated by mechanical shearing and porous media shearing, respectively. In this study, we: (1) analyzed the shear resistance of the copolymers from the perspective of their molecular structure based upon their hydrodynamic radius, weight-average molecular weight, and microstructure; and (2) researched the macro-rheological property and dynamic viscoelasticity of the copolymer before/after shearing to assess the shear stability of the copolymer solution [10]. Finally, indoor mobility control experiments were carried out on the copolymer that was found to have better shear stability in terms of viscosity and rheological property to further investigate its feasibility for enhance oil recovery (EOR).

2. Materials and Methods

2.1. Reagents and Materials

Modified nano-SiO_2 was prepared by the method provided in the references [25]. Acrylamide (AM), acrylic acid (AA), absolute ethyl alcohol (C_2H_5OH), ammonium persulfate ($(NH_4)_2S_2O_8$), sodium hydrogen sulfite ($NaHSO_3$), sodium hydroxide (NaOH), NaCl, $MgCl_2 \cdot 6H_2O$, $CaCl_2$, and other chemicals were purchased from Chengdu KeLong Chemical Reagent Co., Ltd. (Chengdu, China), were of analytical grade, and used without further purification. Partially hydrolyzed polyacrylamide (HPAM, 10% degree of hydrolysis, $M_w = 1.2 \times 10^7$) was obtained from Sichuan Guangya Polymer Chemical Co., Ltd. (Chengdu, China).

2.2. Synthesis of Modified Nano-SiO_2/AA/AM Copolymer

A certain amount of modified nano-SiO_2 (degree of modification: 26% and 38% corresponding to HPMNS-1 and HPMNS-2, respectively), AA, and AM were placed in a 100 mL three-necked flask. An appropriate amount of distilled water was added into the flask to prepare an aqueous solution with monomers having a mass concentration of 26%. After that, the pH value of the solution was

adjusted to 7.4 with sodium hydroxide. Then, ammonium persulfate solution and sodium hydrogen sulfite solution (molar ratio: 1:1) were added into the flask. Copolymerization was performed at 40 °C under nitrogen atmosphere for an indicated time. Finally, modified nano-SiO_2/AA/AM copolymer (HPMNS) was obtained by washing (with absolute ethyl alcohol), smashing, and drying the reaction products. The synthesis route of the copolymer is shown in Scheme 1.

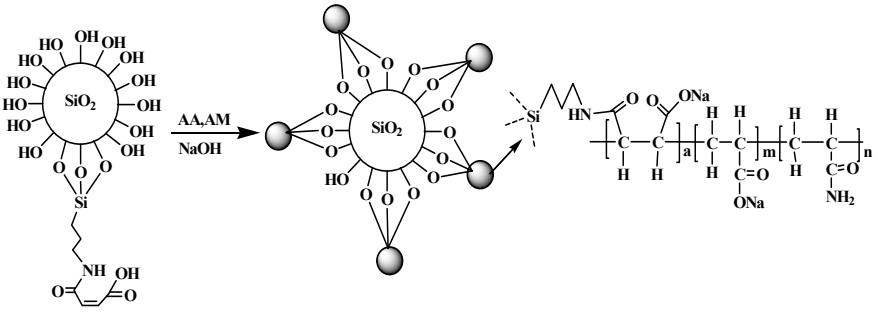

Scheme 1. The synthesis route of modified nano-SiO_2/AA/AM copolymer (HPMNS).

2.3. Characterization

Infrared (IR) spectra of the HPMNS were measured with KBr pellets using a Perkin Elmer RX-1 spectrophotometer (Beijing Rayleigh Analytical Instrument, Beijing, China) in the optical range of 4400–500 cm^{-1}. ^{1}H-NMR and ^{13}C-NMR were recorded on Bruker AC-E 200 spectrometer (Bruker BioSpin, Faellanden, Switzerland) at 400 MHz with D_2O and CCl_4 solvent, respectively. The hydrodynamic diameter (R_h) and distribution of the samples were obtained using a BI-200SM wide-angle dynamic laser light scattering (DLS) instrument. Static laser scattering (SLS) measured the weight-average molecular weight (M_w) and radius of gyration (R_g) of the polymers with the concentration of 30–70 mg/L. The morphologies of the samples before/after shearing were observed by Quanta 450 Environment Scanning Electron Microscope (ESEM, FEI Company, Hillsboro, OR, USA).

2.4. Shear Resistance Test

Polymer (HPAM, HPMNS-1, and HPMNS-2) was dissolved to 2000 mg/L by the brine, whose components are listed in Supplementary Materials, Table S1. The viscosity of HPMNS was determined at different shearing rates on HAAKE RS 600 rotational rheometer at 70 °C. Moreover, the polymer solutions were sheared at different shear strengths by a Mixing Speed Governor (WT-VSA2000B) and different flow rates by a porous media shearing model (inner diameter: 0.01 m; length: 0.235 m; packing: 80–100 mesh quartz sand), which were employed to simulate the mechanical shear degradation of the pipeline and wellbore, and the shear of porous media, respectively. Then the viscosity of the sheared and unsheared polymer solutions was detected by Brookfield DV-III viscometer at 70 °C.

2.5. Rheological Property

The macro-rheological properties of polymer solutions (2000 mg/L by the brine) before/after being sheared by the Mixing Speed Governor (3600 r/min, 20 s) and porous media shearing model (injection speed: 40.4 mL/min) were measured by a HAAKE RS 600 rotational rheometer at 70 °C. The shearing rate was 0.01–400.00 s^{-1} and the measurement duration was 6 min. Simultaneously, HAAKE RS 600 was employed to determine the elastic modulus (G') and viscous modulus (G") of the samples in order to obtain their viscoelasticity properties.

2.6. Mobility Control Capacity

The sand-packed tube displacement experiments were carried out as described in reference [26]. The tubes (30 cm in length and 2.5 cm in inner diameter) were packed with 100–120 mesh quartz sand

that was washed with an 18% hydrochloric acid solution and then with a massive amount of water until the pH reached 7. The brine with a TDS (total dissolved salt) of 9784 mg·L^{-1} was used in the experiments whose ionic composition is shown in Supplementary Materials, Table S1. The flooding rate for water flooding and polymer flooding was set as 1.0 mL/min and kept unchanged. The mobility control ability of polymer was characterized by resistance factor (RF) and residual resistance factor (RRF). The RF and the RRF were calculated by the following equations [22,27]:

$$\mathrm{RF} = \frac{\lambda_w}{\lambda_p} = (\frac{K_w}{\mu_w})/(\frac{K_p}{\mu_p}) \quad (1)$$

$$\mathrm{RFF} = \frac{\lambda_w}{\lambda_p} = (\frac{Q_w}{Q_{wa}})(\frac{\Delta P_{wa}}{\Delta P_w}) \quad (2)$$

where K_w and K_p are the aqueous and polymer phase permeability, respectively ($\times 10^{-3}$ μm^2), μ_w and μ_p are the aqueous and polymer viscosity, respectively (mPa·s), and K_{wb} and K_{wa} are the aqueous phase permeability before and after polymer flooding, respectively, where $K_{wb} = K_W$ ($\times 10^{-3}$ μm^2).

3. Results and Discussion

3.1. IR Spectra, ^{1}H-NMR Spectra, and ^{13}H-NMR Spectra Analysis

The structure of HPMNS was confirmed by IR spectra, as shown in Figure 1a. In the spectrum curve of the copolymer, the peak at 1115 cm^{-1} and 785.2 cm^{-1} were attributed to the antisymmetric stretching vibration and symmetrical stretching vibration of Si–O–Si, respectively. The peak at 3419.7 cm^{-1} was attributed to the stretching vibration peak of N–H. The peak at 2940.6 cm^{-1} was assigned to the stretching vibration of C–H in the methylene. The peaks at 1672.2 cm^{-1} were the stretching vibration peaks of C=O. The results show that the target copolymer was successfully synthesized.

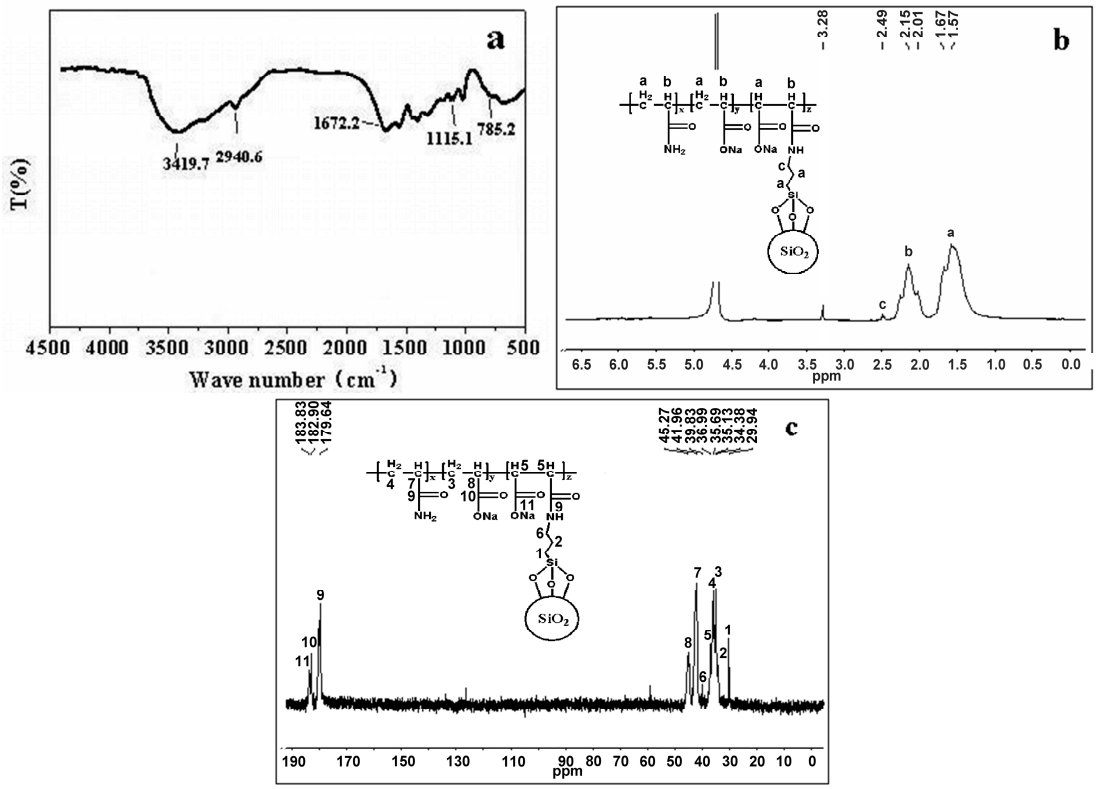

Figure 1. (**a**) IR spectra; (**b**) ^{1}H-NMR spectra; (**c**) ^{13}C-NMR spectra of HPMNS.

Figure 1b shows the ^{1}H NMR spectrum of HPMNS. The chemical shift value at 1.57 ppm was assigned to the methylene (–C***H***$_2$–) protons in the polymeric main chain (–C***H***$_2$–CH(COONa)–, –C***H***$_2$–CH(CONH$_2$)–, –C***H***(COONa)–CH(CONH–)–), and the parts of the modified nano-SiO$_2$ (–C***H***$_2$–C***H***$_2$–CH$_2$(CONH)–), respectively. The chemical shift value at 2.11 ppm was due to the methyne (–C***H***–) protons in the polymeric main chain (–CH$_2$–C***H***(COONa)–, –CH$_2$–C***H***(CONH$_2$)–, and –CH(COONa)–C***H***(CONH–)–). The peak at 2.49 ppm identified the methylene (–C***H***$_2$–) protons on the part attaching to the acylamino of the modified nano-SiO$_2$ (–CH$_2$–CH$_2$–C***H***$_2$(CONH)–).

The ^{13}C-NMR spectrum of HPMNS is shown in Figure 1c. The peaks at 29.94 ppm, 34.38 ppm, and 39.83 ppm were assigned to the carbon in the modified nano-SiO$_2$ (–***C***H$_2$–***C***H$_2$–***C***H$_2$(CONH)–), successively. The chemical shift value at 35.13 ppm, 45.27 ppm, and 182.90 ppm were the part of acrylic acid in the polymeric main chain (–***C***H$_2$–***C***H(***C***OONa)–), successively. The peak at 35.69 ppm, 41.96 ppm, and 179.64 ppm were the part of acrylamide in the polymeric main chain (–***C***H$_2$–***C***H(***C***ONH$_2$)–), successively. The peak at 36.99 ppm was the part of modified nano-SiO$_2$ in the polymeric main chain (–***C***H(COONa)–***C***H(CONH–)–). The chemical shift value at 179.64 ppm was due to the carbon of the acylamino in the modified nano-SiO$_2$ (–CH(COONa)–CH(***C***ONH–)–). Finally, the peak at 183.83 ppm was attributable to carbon of the carboxyl in the modified nano-SiO$_2$ (–CH(***C***OONa)–CH(CONH–)–). Hence, the structure of HPMNS was in accordance with the anticipated polymer molecular structure based on the ^{1}H-NMR and ^{13}C-NMR data.

3.2. Weight-Average Molecular Weight and Flexibility of HPMNS

The weight-average molecular weight and radius of gyration of polymer solutions were determined through a static light scattering test. Figure S1a–c (Supplementary Materials) show Zimm plots of HPAM, HPMNS-1, and HPMNS-2, respectively. On the basis of fundamentals of molecular weight determination by static light scattering, the weight-average molecular weight and radius of gyration of polymers are shown in Table 1.

Table 1. Structural parameters of polymers.

Polymer	Molecular Weight (10^7 g/mol)	Radius of Gyration (nm)	Unperturbed Dimension (nm(mol/g)$^{1/2}$)
HPAM [1]	1.24	129	0.090
HPMNS-1	1.10	117	0.086
HPMNS-2	1.02	96	0.074

[1] HPAM: partially hydrolyzed polyacrylamide.

The flexibility of the polymers' molecular chain was characterized by the unperturbed dimension of the polymers. The unperturbed dimension of the polymers was obtained based upon their radius of gyration and molecular weight according to Equations (1) and (2) [28], as shown in Table 1.

$$A = \sqrt{\langle h^2 \rangle_0 / M} \tag{3}$$

where A is unperturbed dimension of polymer (nm(mol/g)$^{1/2}$), $\langle h^2 \rangle_0$ is mean square end-to-end distance, (nm^2), and M is molecular weight of polymer (g/mol).

The unperturbed dimension of polymer represents the unperturbed mean square end-to-end distance of unit molecular weight which cannot be directly measured, but the mean square radius of gyration $\left\langle {R_g}^2 \right\rangle$, which is used to characterize the molecular dimension, can be directly measured by experiment. Mathematical justification showed that when the molecular weight is infinite, the relationship between the mean square end-to-end distance and mean square radius of gyration of the freely jointed chain and equivalent freely jointed chain are as follows:

$$\langle R_g{}^2 \rangle = \frac{1}{6}\langle h^2 \rangle_0 \quad (4)$$

where $\left\langle R_g{}^2 \right\rangle$ is mean square radius of gyration (nm^2).

In Table 1, among the three polymers, HPMNS-2 had the highest flexibility, followed by HPMNS-1 and HPAM. This result is due to the molecular chains of HPAM comprising a C–C single bond. In the modified nano-SiO_2/AA/AM copolymer, the 3-aminopropyl trimethoxysilane molecular structure used for nano-SiO_2 modification contains a C–Si single bond and C–N single bond, which have fewer barriers to internal rotation compared with the C–C single bond, thus resulting in easier conformational transitions and more conformations [29]. Similarly, because of a higher degree of modification, the proportion of C–Si single bonds and C–N single bonds in the molecular chains of HPMNS-2 was higher than that of HPMNS-1.

3.3. Hydrodynamic Radius of HPMNS

The hydrodynamic radius of HPAM (281 nm), HPMNS-1 (198 nm), and HPMNS-2 (163 nm) are shown in Figure S2a–c (Supplementary Materials), respectively. Compared to HPAM, which was of linear structure and existed in the solution in the form of random molecular coil, HPMNS, which was of hyperbranched structure with a network structure in the solution, had more contracted conformations. Hence, HPMNS had a shorter hydrodynamic radius than HPAM. In addition, HPMNS-2 has a higher degree of modification, more branched chains, lower molecular weight, and finer structure than HPMNS-1, thus its hydrodynamic radius was the shortest.

3.4. Shear Resistance of HPMNS

During the injection process, the polymer viscosity will decrease owing to shear degradation occurred in injection pipelines, equipment, perforation nozzles, and near well bore [12]. Hence, we needed to carry out experimental evaluations for the shear resistance of polymers.

In this study, the shear recovery curve of the copolymer is shown in Figure 2. The viscosity retention ratio of HPMNS solution was 84.9% after it was sheared at the speed of 500 s^{-1} for 5 min. This indicated that the copolymer had some shear resistance.

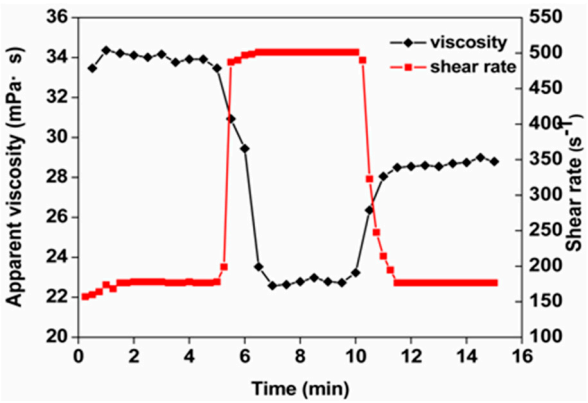

Figure 2. Shear recovery curve of HPMNS.

The viscosity retention ratios of polymer solutions sheared by the Mixing Speed Governor at diverse shear strengths are shown in Table 2. Compared with HPAM solution, HPMNS possessed higher viscosity retention ratios under the same conditions, and as the shearing strength increased, the decreasing trend of the viscosity retention ratio of HPMNS decreased. Thus, HPMNS showed some shear resistance. Moreover, HPMNS-2 with a higher degree of modification, had better shear resistance.

Table 2. Viscosity retention ratios of polymer solutions sheared by the Mixing Speed Governor.

Polymer	Viscosity before Shearing (mPa·s)	3600 r/min for 20 s		7200 r/min for 20 s		11,000 r/min for 20 s	
		Viscosity (mPa·s)	Retention Ratio (%)	Viscosity (mPa·s)	Retention Ratio (%)	Viscosity (mPa·s)	Retention Ratio (%)
HPAM	24.6	11.1	45.12	9.1	36.99	5.5	22.36
HPMNS-1	34.2	17.2	50.29	14.9	43.57	10.2	29.82
HPMNS-2	32.1	17.4	54.21	15.3	47.66	10.9	33.96

As shown in Table 3, the shearing by porous media had great impacts on the viscosity of polymer solutions. The higher the injection velocity was, the lower the viscosity retention ratio of polymer solutions was. The viscosity retention ratio of HPAM was 53.25% at an injection velocity of 40.4 mL/min. When the velocity was increased to 80.8 mL/min, the viscosity retention ratio was as low as 28.46%. Nevertheless, compared with HPAM solution, HPMNS enjoyed higher viscosity retention ratios under the same conditions. Besides, HPMNS-2 showed better shear resistance with a viscosity retention ratio of 60.12%, while that of HPMNS-1 and HPAM was 58.48% and 53.25%, respectively, at a fixed injection velocity of 40.4 mL/min.

Table 3. Viscosity retention ratios of polymer solutions sheared by the porous media shearing model.

Polymer	Viscosity before Shearing (mPa·s)	40.4 mL/min		60.6 mL/min		80.8 mL/min	
		Viscosity (mPa·s)	Retention Ratio (%)	Viscosity (mPa·s)	Retention Ratio (%)	Viscosity (mPa·s)	Retention Ratio (%)
HPAM	24.6	13.1	53.25	10.2	41.46	7.0	28.46
HPMNS-1	34.2	20.0	58.48	16.3	47.66	12.2	35.67
HPMNS-2	32.1	19.3	60.12	16.0	49.84	12.3	38.32

According to the above results, HPMNS-2 showed the best shear resistance, followed by HPMNS-1 and HPAM, to mechanical shear action and porous media shear action. From the perspective of molecular structure, owing to their having the highest flexibility, the molecular chains of HPMNS-2 could deform according to the pore-throat size when the polymer solutions flowed through porous media, thus suffering from less damage than HPMNS-1 and HPAM at the same degree of blockage. Similarly, the molecular chain conformations of HPMNS-2 solution were contracted due to this molecule's short hydrodynamic radius. The proportion of its damaged molecular chains decreased, and the impact of shear action on hydrodynamic radius was reduced. In addition, when the hydrodynamic radius was small, it was easier for the solutions to flow through the pore throat of porous media. Therefore, the viscosity retention ratios of HPAM, HPMNS-1, and HPMNS-2 solutions rose successively after they were sheared by the Mixing Speed Governor and porous media.

3.5. Morphology of HPMNS

To investigate microstructures of HPAM, HPMNS-1, and HPMNS-2, ESEM was utilized on unsheared and sheared (by the Mixing Speed Governor) polymer solutions. As can be seen from Figure 3a, before shearing, vast molecular coils were entangled with each other, thus forming some network structures in HPAM solution. After shearing, the coil size reduced and the network structures in the solution became weaker (Figure 3b). On the contrary, finer network structures were formed in HPMNS-1 and HPMNS-2 sheared solutions (as shown in Figure 3d,f), which was beneficial for enhancing the acting force among molecular chains and protecting molecular chains from being more damaged. This phenomena is due to the hyperbranched structures of HPMNS in solution; the coil size of the molecule was reduced, but the molecular coils were still entangled after shearing. Therefore, HPMNS had higher viscosity retention ratios than HPAM under the same shear strength.

The network structures in HPMNS-2 solution were more compact than those in HPMNS-1 due to a higher degree of modification. HPMNS-2 had more branched chains, which were beneficial for

enhancing the acting force among molecular chains and consequently intensifying the entanglement of molecular chains. In addition, HPMNS-2 had a shorter hydrodynamic radius, more contracted conformations, and a lower proportion of damaged molecular chains at the same shear strength, which could form more compact network structures after shearing. This accounts for the better shearing resistance of HPMNS-2 compared with HPMNS-1.

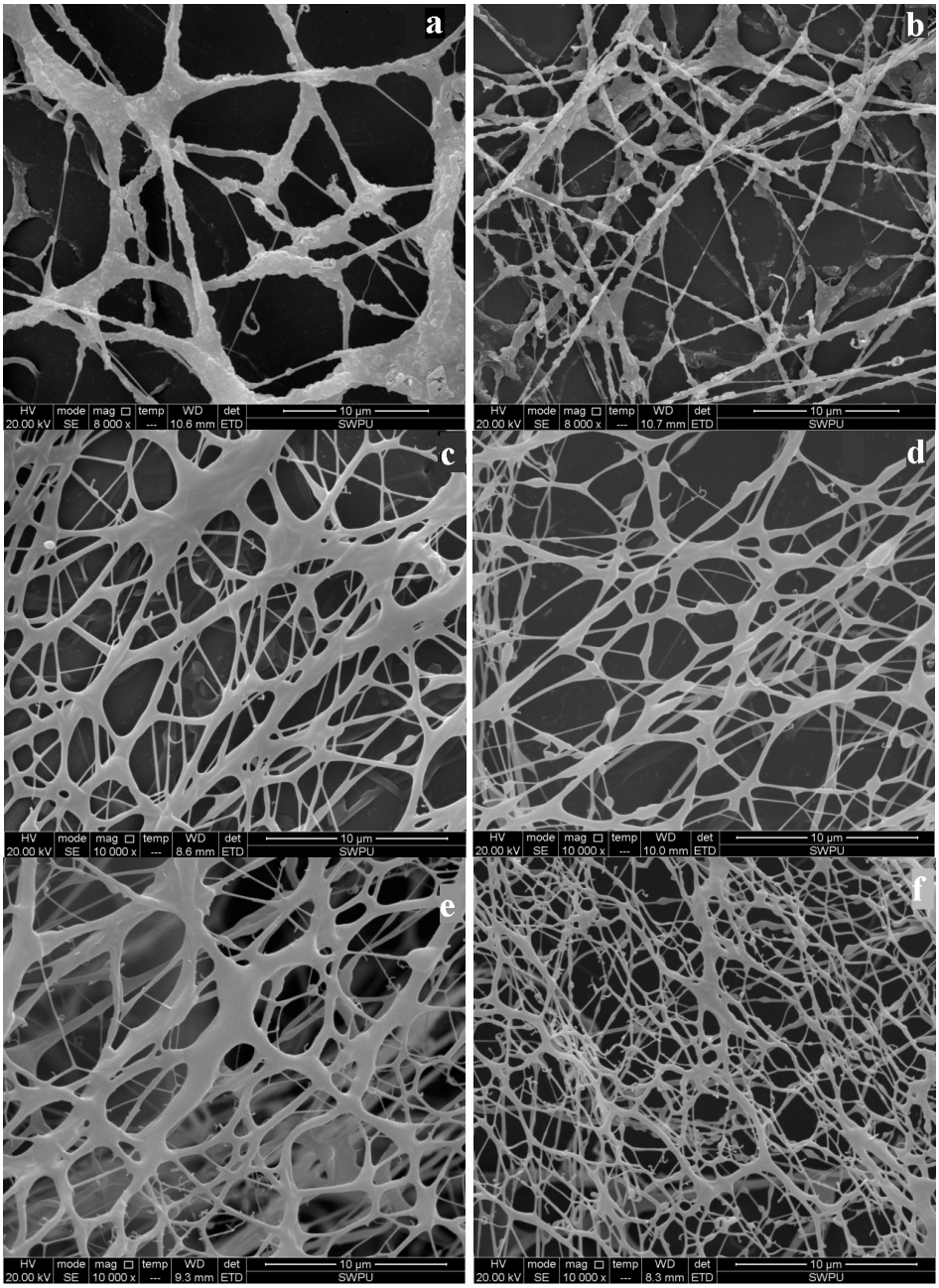

Figure 3. Environment scanning electron microscope (ESEM) images of (**a**) HPAM-unsheared; (**b**) HPAM-sheared; (**c**) HPMNS-1-unsheared; (**d**) HPMNS-1-sheared; (**e**) HPMNS-2-unsheared; (**f**) HPMNS-2-sheared.

3.6. Rheological Property of HPMNS

The rheological behavior of a polymer solution is very important for its application in enhanced oil recovery [9]. With a good viscoelastic performance, the polymer can effectively displace small

oil blocks in the dead angles of formation [30]. Hence, from the perspective of rheological behavior, we assessed the shear stability of HPMNS by studying the macro-rheological property and dynamic viscoelasticity of sheared and unsheared polymer solutions.

The variation of the apparent viscosity was curved based on the shearing rate, as shown in Figure 4. HPMNS and HPAM solutions before (Figure 4a) and after shearing (Figure 4b,c) all showed shear-thinning behaviors, which is beneficial from the standpoint of injectivity. Because the viscosity near the injection well is lower due to higher shear rate, there is a more favorable injectivity. Once the polymer moves far into the reservoir, shear rates decline and the viscosity increases, which provides the desired mobility control [31].

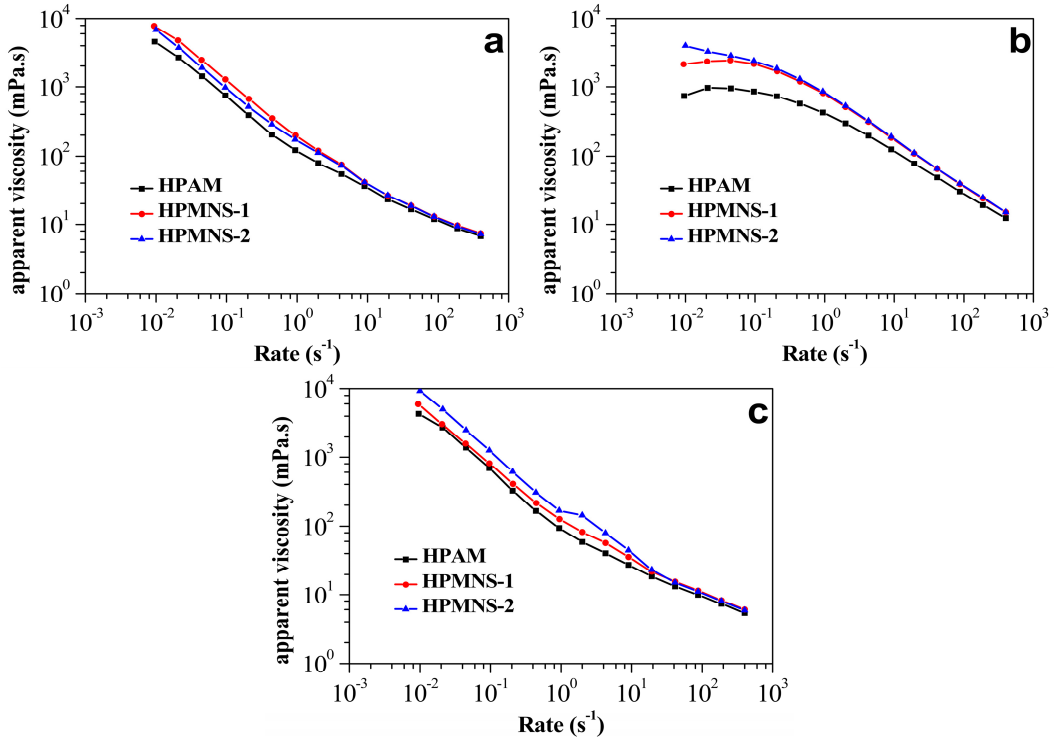

Figure 4. Macro-rheological properties of (**a**) unsheared; (**b**) sheared by the Mixing Speed Governor, and (**c**) polymer solutions 'sheared by porous media shearing model.

At low shearing rates, the viscosities of the sheared and unsheared HPMNS solutions were all higher than those of HPAM. This was due to HPMNS being a hyperbranched polymer that can form stronger structures in the solution. In addition, with good shear resistance, the impact of shear action on HPMNS solution viscosity was less than HPAM, giving it better stability in terms of rheological behavior after being sheared by the Mixing Speed Governor and porous media shearing model.

Compared with HPMNS-2, the unsheared HPMNS-1 solution had higher viscosities at low shearing rates. The cause might be that the conformational changes of molecular chains in the polymers were very slow when the shearing rates were low, as they needed to overcome great internal frictional resistance. On the other hand, HPMNS-1 and HPMNS-2 had similar structures before shearing. Under this circumstance, the larger the hydrodynamic radius was, the higher the internal frictional resistance was. Thus, having the higher molecular weight and larger hydrodynamic radius, HPMNS-1 solution had higher viscosity. This phenomenon was opposite in the sheared solution, where HPMNS-2 had higher viscosity than HPMNS-1 at low shearing rates, as shown in Figure 4b,c. This could be attributed to HPMNS-2 having a better shear resistance.

The dynamic viscoelasticity of the polymer solutions is shown in Figure 5 (scanning stress: 0.10 Pa, scanning frequency: 0.1–15.0 Hz). At the scanning frequency of 0.1–4.6 Hz, the viscosity modulus (G″)

of the sheared and unsheared polymer solutions were all higher than its elasticity modulus (G′), which was dominated by viscosity. From Figure 5a, the values of G′ and G″ of unsheared HPMNS-1 solution were both higher than those of HPMNS-2, followed by those of HPAM. With better shearing resistance, HPMNS-2 could be comparable to HPMNS-1 in terms of viscosity modulus and elasticity modulus, after being sheared by the Mixing Speed Governor (Figure 5b). When passing through the pore throat of porous media, HPMNS-2 was more flexible than HPMNS-1, since it could deform and then recover to some extent. By this way, the values of G′ and G″ for HPMNS-2 increased (Figure 5c).

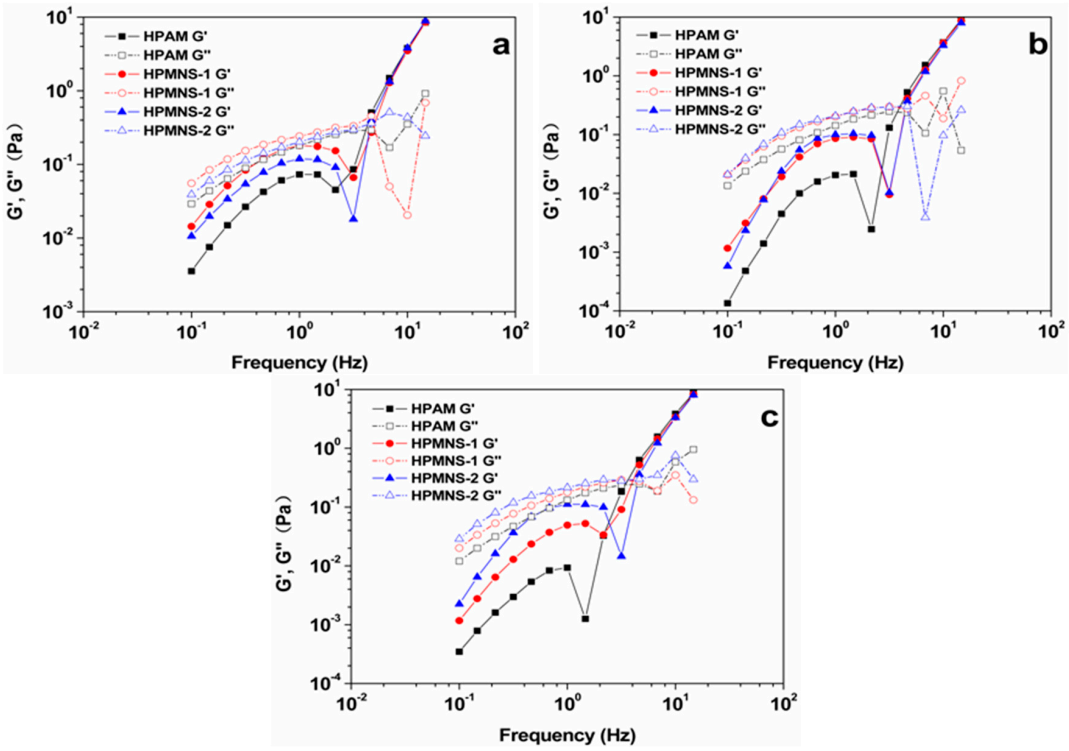

Figure 5. Dynamic viscoelasticity of (**a**) unsheared (**b**) sheared by the Mixing Speed Governor; and (**c**) polymer solutions sheared by porous media shearing model.

3.7. Mobility Control Capacity of HPMNS

The basic idea behind using water-soluble polymers in many oilfield operations and various enhanced oil recovery processes is to reduce the mobility of the aqueous phase and consequently to improve the sweep efficiency [32,33]. Due to the good thickening ability of the sheared HPMNS-2 solution, reduction of the water–oil mobility ratio can be achieved by increasing the viscosity of the water phase [27]. Furthermore, on the basis of mobility control theory, increasing the residual resistance factor not only reduces the water–oil mobility ratio, but also decreases the requirement for viscosity enhancement of the polymer solution [34]. In view of this, we studied the residual resistance factor caused by HPMNS-2, which had better shear stability than HPMNS-1, to investigate its feasibility for EOR.

With a permeability of K = 300 × 10^{-3} μm^2, the injection pressure curves of HPMNS-2 and HPAM solution in different concentrations (1000, 2000 mg/L) are shown in Figure 6. In an oil reservoir with a permeability of K = 300 × 10^{-3} μm^2, the injection pressures of the copolymer, with concentrations of 1000 mg/L and 2000 mg/L, were less than 0.6 MPa and 1.8 MPa, respectively. The polymer solution was injected after the differential pressure of water flooding became stable and the water-phase permeability was determined. The differential pressure increased rapidly at the beginning and then slowed down. After the differential pressure became stable again, we started water flooding. At this

time, the differential pressure fell rapidly and finally became stable. This means that the copolymer solutions had good injectivity in a low-to-medium permeability oil reservoir. As the injection increased, the pressure at the inlet of the homogeneous model rose gently, and reached the peak when the injection volume was about 15 PV. Thereafter, the injection pressure fell to a steady level. It can be seen from the study that the polymer solutions had good mobility control capacities in the porous media with a low-to-medium permeability.

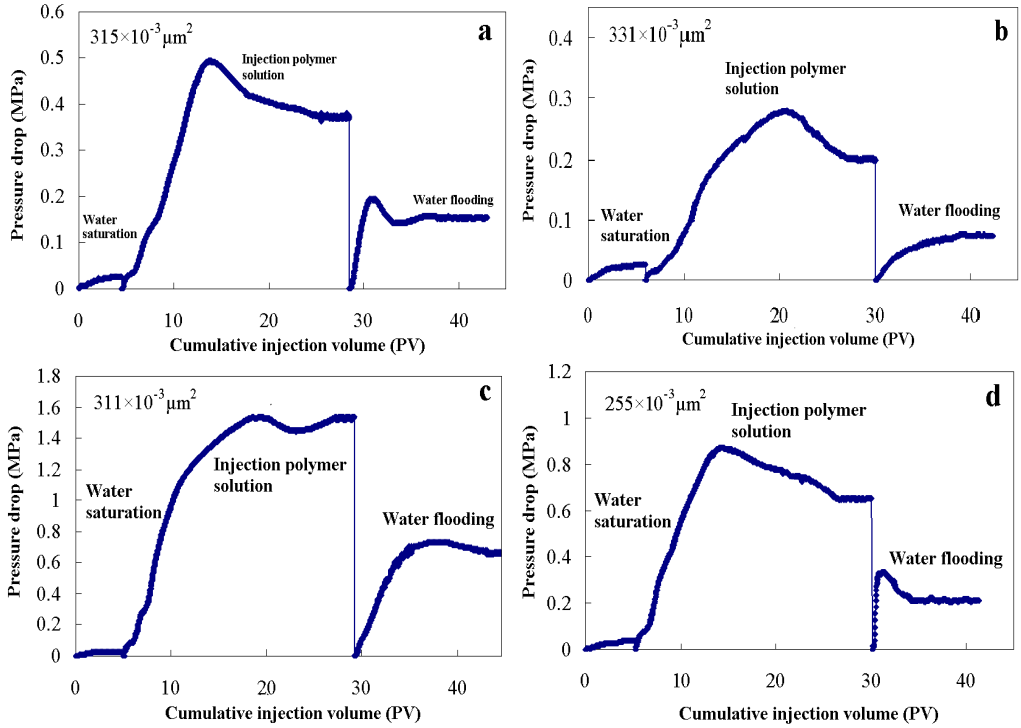

Figure 6. Flow characteristic curves of HPMNS-2 solution at a concentration of (**a**) 1000 mg/L and (**c**) 2000 mg/L, and HPAM solution at a concentration of (**b**) 1000 mg/L and (**d**) 2000 mg/L.

The RF and RFF of polymer solutions were calculated according to the data of the injection pressure curves, as shown in Table 4. The RF and the RFF of HPMNS-2 solutions (1000 mg/L and 2000 mg/L) were both higher than those of HPAM under the same conditions. This means that polymer solutions could establish higher RF and RFF and had a stronger mobility control capacity that was favorable to enhanced oil recovery.

Table 4. Resistance factor and residual resistance factor of polymer solutions.

Polymer	Permeability ($\times 10^{-3}$ μm^2)	Concentration (mg/L)	Apparent Viscosity (mPa·s)	Resistance Factor	Residual Resistance Factor
HPMNS-2	315	1000	14.4	13.8	5.7
HPAM	331	1000	5.2	7.5	2.8
HPMNS-2	311	2000	25.1	56.4	24.4
HPAM	255	2000	8.9	15.6	5.0

4. Conclusions

The modified nano-SiO_2/AA/AM copolymer was synthesized by free-radical polymerization. Fourier-transformation infrared (FTIR), ^{1}H-NMR and ^{13}C-NMR, DLS, SLS, and ESEM measurements confirmed its chemical structure and morphology. The experiments with different shearing models convincingly proved that compared with HPAM, which has been widely used in EOR,

the hyperbranched structure provided the modified nano-SiO_2/AA/AM copolymers with excellent shear resistance. From a microstructural point, the observation results of ESEM showed that the damage to molecular chains of the copolymer caused by shearing was less. Moreover, the higher the degree of modification was, the better shear resistance there was. The rheological properties of HPMNS solutions showed shear-thinning behavior, and sheared HPMNS-2 solutions had the highest viscosity at a low shearing rate. At a scanning stress of 0.10 Pa, the viscoelasticity of both HPMNS copolymers before/after shearing were higher than that of HPAM. Furthermore, compared to HPAM, the copolymers could establish higher RF and RFF in a medium-porous medium under a similar permeability, and had stronger mobility control capacity that could effectively improve the EOR.

Supplementary Materials: The following are available online at www.mdpi.com/1996-1073/9/12/1037/s1. Figure S1: Zimm plot of (a) HPAM; (b) HPMNS-1; (c) HPMNS-2, Figure S2: Hydrodynamic radius of (a) HPAM; (b) HPMNS-1; and (c) HPMNS-2, Table S1: The component of the seminiferous water.

Acknowledgments: This work was supported financially by the National Natural Science Foundation of China (Grant No. 51404208), the China Scholarship Council, the second Youth Backbone Teachers Project of Southwest Petroleum University, the Open Fund (PLN1433) of the State Key Laboratory of Oil and Gas Reservoir Geology and Exploitation (Southwest Petroleum University), the National Undergraduate Training Programs for Innovation and Entrepreneurship (Grant No. 201510615008), the Scientific research project of Southwest Petroleum University (Grant No. 2014QHZ014), the Undergraduate Extracurricular Open Experiment of Southwest Petroleum University (KSZ15070).

Author Contributions: Nanjun Lai, Xin Guo conceived the idea of the modified Nano-SiO_2/AA/AM copolymer oil displacement agent and contributed to the discussion of the results; Xin Guo, Ning Zhou and Qian Xu performed the experiments; Nanjun Lai and Xin Guo wrote the paper; all authors have read and approved the final manuscript.

Conflicts of Interest: The authors declare no conflict of interest.

References

1. Wassmuth, F.R.; Arnold, W.; Green, K.; Cameron, N.J. Polymer Flood Application to Improve Heavy Oil Recovery at East Bodo. *J. Can. Pet. Technol.* **2009**, *48*, 55–61. [CrossRef]
2. Muhammad, S.K.; Abdullah, S.S.; Usamah, A.A.; Ibnelwaleed, A.H. Review on Polymer Flooding: Rheology, Adsorption, Stability, and Field Applications of Various Polymer Systems. *Polym. Rev.* **2015**, *55*, 491–530.
3. Alvarado, V.; Manrique, E. Enhanced Oil Recovery: An Update Review. *Energies* **2010**, *3*, 1529–1575. [CrossRef]
4. Wever, D.A.Z.; Picchioni, F.; Broekhuis, A.A. Polymers for Enhanced Oil Recovery: A Paradigm for Structure-property Relationship in Aqueous Solution. *Prog. Polym. Sci.* **2011**, *36*, 1558–1628. [CrossRef]
5. Jung, J.C.; Zhang, K.; Chon, B.H.; Choi, H.J. Rheology and Polymer Flooding Characteristics of Partially Hydrolyzed Polyacrylamide for Enhanced Heavy Oil Recovery. *J. Appl. Polym. Sci.* **2013**, *127*, 4833–4839. [CrossRef]
6. Wang, J.; Dong, M. Optimum Effective Viscosity of Polymer Solution for Improving Heavy Oil Recovery. *J. Pet. Sci. Eng.* **2009**, *67*, 155–158. [CrossRef]
7. Ye, M.L.; Han, D.; Shi, L.H. Studies on Determination of Molecular Weight for Ultrahigh Molecular Weight Partially Hydrolyzed Polyacrylamide. *J. Appl. Polym. Sci.* **1996**, *60*, 317–322. [CrossRef]
8. Zhu, D.; Wei, L.; Wang, B.; Feng, Y. Aqueous Hybrids of Silica Nanoparticles and Hydrophobically Associating Hydrolyzed Polyacrylamide Used for EOR in High-Temperature and High-Salinity Reservoirs. *Energies* **2014**, *7*, 3858–3871. [CrossRef]
9. Samanta, A.; Bera, A.; Ojha, K.; Mandal, A. Effects of Alkali, Salts, and Surfactant on Rheological Behavior of Partially Hydrolyzed Polyacrylamide Solutions. *J. Chem. Eng. Data* **2010**, *55*, 4315–4322. [CrossRef]
10. Tolstikh, L.I.; Akimov, N.L.; Golubeva, I.A.; Shvetsov, I.A. Degradation and Stabilization of Polyacrylamide in Polymer Flooding Conditions. *Int. J. Polym. Mater.* **1992**, *17*, 177–193. [CrossRef]
11. Al-Hashmi, A.A.; Al-Maamari, R.; Al-Shabibi, I.; Mansoor, A.; Al-Sharji, H.; Zaitoun, A. Mechanical Stability of High-Molecular-Weight Polyacrylamides and an (acrylamido tert-butyl sulfonic acid)–Acrylamide Copolymer Used in Enhanced Oil Recovery. *J. Appl. Polym. Sci.* **2014**, *20*, 40921.
12. Zaitoun, A.; Makakou, P.; Blin, N.; Al-Maamari, R.S.; Al-Hashmi, A.A.R.; Abdel-Goad, M. Shear Stability of EOR Polymers. In Proceedings of the SPE International Symposium on Oilfield Chemistry, The Woodlands, TX, USA, 11–13 April 2011.

13. Seright, R.S. The Effects of Mechanical Degradation and Viscoelastic Behavior on Injectivity of Polyacrylamide Solutions. *SPE J.* **1983**, *23*, 475–485. [CrossRef]
14. Xue, L.; Agarwal, U.S.; Lemstra, P.J. Shear Degradation Resistance of Star polymers During Elongational Flow. *Macromolecules* **2005**, *38*, 8825–8832. [CrossRef]
15. Maghzi, A.; Mohebbi, A.; Kharrat, R.; Ghazanfari, M.H. An Experimental Investigation of Silica Nanoparticles Effect on the Rheological Behavior of Polyacrylamide Solution to Enhance Heavy Oil Recovery. *Pet. Sci. Technol.* **2013**, *31*, 500–508. [CrossRef]
16. Caulfield, M.J.; Qiao, G.G.; Solomon, D.H. Some Aspects of the Properties and Degradation of Polyacrylamides. *Chem. Rev.* **2002**, *102*, 3067–3083. [CrossRef] [PubMed]
17. Tomalia, D.A.; Uppuluri, S.; Swanson, D.R.; Li, J. Dendrimers as Reactive Modules for the Synthesis of New Structure-Controlled, Higher complexity Megamers. *Pure Appl. Chem.* **2000**, *72*, 2343–2358. [CrossRef]
18. Tomalia, D.A.; Baker, H.; Dewald, J. New Class of Polymers: Starburst-dendritic Macromolecules. *Polym. J.* **1984**, *17*, 117–132. [CrossRef]
19. Lai, N.; Zhang, Y.; Wu, T.; Zhou, N.; Liu, Y.; Ye, Z. Effect of Sodium Dodecyl Benzene Sulfonate to the Displacement Performance of Hyperbranched Polymer. *Russ. J. Appl. Chem.* **2016**, *89*, 70–79. [CrossRef]
20. Schull, C.; Frey, H. Grafting of Hyperbranched Polymers: From Unusual Complex Polymer Topologies to Multivalent Surface Functionalization. *Polymer* **2013**, *54*, 5443–5455. [CrossRef]
21. Percy, M.J.; Barthet, C.; Lobb, J.C.; Khan, M.A.; Lascelles, S.F.; Vamvakaki, M.; Armes, S.P. Synthesis and Characterization of Vinyl Polymer-Silica Colloidal Nanocomposites. *Langmuir* **2000**, *16*, 6913–6920. [CrossRef]
22. Ponnapati, R.; Karazincir, O.; Dao, E.; Ng, R.; Mohanty, K.K.; Krishnamoorti, R. Polymer-Functionalized Nanoparticles for Improving Waterflood Sweep Efficiency: Characterization and Transport Properties. *Ind. Eng. Chem. Res.* **2011**, *50*, 13030–13036. [CrossRef]
23. Pu, W.F.; Liu, R.; Wang, K.Y.; Li, K.X.; Yan, Z.P.; Li, B.; Zhao, L. Water-Soluble Core−Shell Hyperbranched Polymers for Enhanced Oil Recovery. *Ind. Eng. Chem. Res.* **2015**, *54*, 798–807. [CrossRef]
24. Xin, H.; Ao, D.; Wang, X.; Zhu, Y.; Zhang, J.; Tan, Y. Synthesis, Characterization, and Properties of Copolymers of Acrylamide With Sodium 2-Acrylamido-2-Methylpropane Sulfonate with Nano Silica Structure. *Colloid Polym. Sci.* **2015**, *293*, 1307–1316. [CrossRef]
25. Lai, N.; Wu, T.; Ye, Z.; Zhou, N.; Zeng, F. Hybrid Hyperbranched Polymer Based on modified Nano-SiO_2 for Enhanced Oil Recovery. *Chem. Lett.* **2016**, *45*, 1189–1191. [CrossRef]
26. Lai, N.; Zhang, Y.; Xu, Q.; Zhou, N.; Wang, H.; Ye, Z. A Water-Soluble Hyperbranched Copolymer Based on a Dendritic Structure for Low-to-Moderate Permeability Reservoirs. *RSC Adv.* **2016**, *6*, 32586–32597. [CrossRef]
27. Maia, A.M.S.; Borsali, R.; Balaban, R.C. Comparison between a Polyacrylamide and a Hydrophobically Modified Polyacrylamide Flood in a Sandstone Core. *Mater. Sci. Eng. C* **2009**, *29*, 505–509. [CrossRef]
28. Thomas, C.A. The Unperturbed Molecular Dimensions of Poly (Ethylene Oxide) in Aqueous Solutions from Intrinsic Viscosity Measurements and the Evaluation of the Theta Temperature. *Polymer* **1982**, *23*, 1775–1779. [CrossRef]
29. Guo, L.M.; Zhao, D.L. *High-Polymer Physics*; Beijing University of Aeronautics and Astronautics Press: Beijing, China, 2005; pp. 33–35.
30. Zou, C.; Gu, T.; Xiao, P.; Ge, T.; Wang, M.; Wang, K. Experimental Study of Cucurbit[7]uril Derivatives Modified Acrylamide Polymer for Enhanced Oil Recovery. *Ind. Eng. Chem. Res.* **2014**, *53*, 7570–7578. [CrossRef]
31. Lee, K.S. Performance of a Polymer Flood with Shear-Thinning Fluid in Heterogeneous Layered Systems with Crossflow. *Energies* **2011**, *4*, 1112–1128. [CrossRef]
32. Giese, S.W.; Powers, S.E. Using Polymer Solutions to Enhance Recovery of Mobile Coal Tar and Creosote DNAPLs. *J. Contam. Hydrol.* **2002**, *58*, 147–167. [CrossRef]
33. Samanta, A.; Ojha, K.; Sarkar, A.; Mandal, A. Mobility Control and Enhanced Oil Recovery Using Partially Hydrolysed Polyacrylamide (PHPA). *Int. J. Oil Gas Coal Technol.* **2013**, *3*, 245–258. [CrossRef]
34. Shi, L.; Ye, Z.; Zhang, Z.; Zhou, C.; Zhu, S.; Guo, Z. Necessity and Feasibility of Improving the Residual Resistance Factor of Polymer Flooding in Heavy Oil Reservoirs. *Pet. Sci.* **2010**, *7*, 251–256. [CrossRef]